
A Benchmark for Maximum Cut: Towards Standardization of the Evaluation of Learned Heuristics for Combinatorial Optimization

Ankur Nath

Texas A&M University
College Station, TX, USA
anath@tamu.edu

Alan Kuhnle

Texas A&M University
College Station, TX, USA
kuhnle@tamu.edu

Abstract

Recently, there has been much work on the design of general heuristics for graph-based, combinatorial optimization problems via the incorporation of Graph Neural Networks (GNNs) to learn distribution-specific solution structures. However, there is a lack of consistency in the evaluation of these heuristics, in terms of the baselines and instances chosen, which makes it difficult to assess the relative performance of the algorithms. In this paper, we propose an open-source benchmark suite **MaxCut-Bench** dedicated to the NP-hard Maximum Cut problem in both its weighted and unweighted variants, based on a careful selection of instances curated from diverse graph datasets. The suite offers a unified interface to various heuristics, both traditional and machine learning-based. Next, we use the benchmark in an attempt to systematically corroborate or reproduce the results of several, popular learning-based approaches, including S2V-DQN [31], ECO-DQN [4], among others, in terms of three dimensions: **objective value**, **generalization**, and **scalability**. Our empirical results show that several of the learned heuristics fail to outperform a naive greedy algorithm, and that only one of them consistently outperforms Tabu Search, a simple, general heuristic based upon local search. Furthermore, we find that the performance of ECO-DQN remains the same or is improved if the GNN is replaced by a simple linear regression on a subset of the features that are related to Tabu Search. Code, data, and pretrained models are available at: <https://github.com/ankurnath/MaxCut-Bench>.

1 Introduction

The design of effective heuristics or approximation algorithms for NP-hard combinatorial optimization (CO) problems is a challenging task, often requiring domain-specific knowledge alongside a rigorous process of empirical refinement. Typically, the precise probability distribution of a particular set of instances that are needed for a given application is complex or unknown, and may deviate far from the set of worst-case instances that give rise to the computational complexity of the problem at hand. For example, consider a shipping company that must solve a presumably similar optimization problem each day for the routing of its delivery vehicles. Consequently, there has been significant interest among researchers in automating this demanding and tedious design process using machine learning to develop algorithms that exploit the inherent structure of these distributions [31, 4, 5, 55, 46]. Empirical evidence suggests that learned heuristics [5, 46] can be competitive with state-of-the-art (SOTA) heuristics specifically tailored to individual problems.

However, along with the surge of automated, general heuristics for CO problems, it is necessary to have a standardized way to evaluate these heuristics to determine what gains, if any, are made over more traditional heuristics. The current status of the field is that each work formulates a heuristic

and then selects its own baselines, problems, and instance distributions to evaluate the heuristic – inevitably, these are ones that showcase the new heuristic in the best possible light. Often, a combination of weak traditional heuristics and expensive exact algorithms are employed as baselines, such as the Greedy algorithm (weak) or exact IP solvers, such as Gurobi [24] and CPLEX [16]. However, moderate-strength heuristics such as local search algorithms or even naive stochastic greedy algorithms are typically omitted. More discussion and details can be found in Appendix A.3.

In this work, we focus on the Maximum Cut problem. Many real-world applications [38, 17, 47] can be reduced to MaxCut. Significant commercial and research efforts have been dedicated to developing MaxCut solvers, based on classical [23] and quantum annealing [33, 44] approaches, as well as classical [22, 7] and learned [4, 5, 55] algorithms. These efforts underscore the combination of intractability and broad applicability that motivates our focus on this problem. We carefully select distributions of instances for MaxCut – then, we evaluate the performance of several highly cited and recently proposed heuristics on these instances. We have the following research questions:

In this setting, can we reproduce or corroborate the performance of learned heuristics as compared to their traditional counterparts? Is there any absolute performance gain with learned heuristics compared to reasonably effective, traditional baselines? Finally, how well do algorithms trained with one distribution generalize to another?

The Maximum Cut (MaxCut) problem is formally defined as follows. Given an undirected graph $G(V, E)$, where V represents the set of vertices, E denotes the set of edges and weights $w(u, v)$ on the edges $(u, v) \in E$, the goal is to find a subset of nodes $S \subseteq V$ that maximizes the objective function, $f(S) = \sum_{u \in S, v \in V \setminus S} w(u, v)$.

Contributions.

- We provide an open-source benchmark suite (**MaxCut-Bench**) for Maximum Cut solvers. The software currently supports several highly cited or recently proposed, learned heuristics such as S2V-DQN [31], ECO-DQN [4], LS-DQN [51], ANYCSP [46], RUN-CSP [45], Gflow-CombOpt [55], CAC [32], and AHC [33]. We reimplemented several learned local search algorithms using modern, more efficient graph learning packages, allowing them to scale up to larger instances. We propose a large and diverse collection of MaxCut instances with best known solution values, including instances that have been used in the past to benchmark SOTA traditional heuristics.
- Using **MaxCut-Bench**, we conduct an evaluation of learned and classical heuristics across multiple datasets. We show that Tabu Search [21], a simple heuristic based upon local search, outperforms all the evaluated learned heuristics in terms of **objective value**, **scalability** and **generalization**, except for ANYCSP. Moreover, a naive reversible greedy algorithm outperforms several of the learned heuristics and is competitive with the popular S2V-DQN algorithm. Due to the wide-ranging solid performance of Tabu Search across all instances, we recommend that it be included as a baseline for any future heuristic claimed to solve MaxCut. ANYCSP, a global search heuristic, is the best performing of the evaluated heuristics, indicating that a reinforcement learning approach to general constraint satisfaction for CO problems is a promising direction for future research.
- Using **MaxCut-Bench**, we show that while combining local search algorithms with deep learning can improve their performance, the good performance of a highly-cited heuristic, ECO-DQN, can be achieved by simply selecting a subset of its features (which are related to Tabu Search) and replacing the GNN with a linear regression model. This result suggests that care should be taken not to conflate the performance added by the GNN with the power of an underlying classical heuristic, such as local search or Tabu Search.

We believe that this benchmark will enable research community to standardize further research endeavors in machine learning for solving CO problems .

Organization. The rest of this paper is organized as follows. In Section 2, we discuss relevant related work. We present the the MaxCut-Bench instance distributions and algorithms in Section 3. In Section 4, we use the benchmark to answer the motivating questions above. Finally, in Section 5, we conclude the paper.

2 Related Work

Alongside the growing interest in GNNs for tackling CO problems, there have been a number of recent works revisiting the effectiveness versus traditional heuristics. Angelini and Ricci-Tersenghi [2] demonstrated that a simple greedy algorithm running almost in linear time can find solutions of better quality than a physics-inspired unsupervised GNN [39] for the Maximum Independent Set (MIS) problem. Similarly, for MIS, Böther et al. [10] demonstrated that the performance of the popular guided tree search algorithm [34] is not reproducible, and the GNN used in the tree search does not play any meaningful role. Rather, the various classical algorithms are the reason for good performance, especially on hard instances. This is analogous to our result for the ECO-DQN algorithm (Section 4.1), where we show that the GNN does not appear to play a meaningful role in the algorithm, and instead, the good performance of ECO-DQN for MaxCut may come from its Tabu Search-related features.

For Boolean Satisfiability, RLSAT [54] was shown to match the performance of the traditional local search algorithm WalkSAT [40]. However, Tönshoff et al. [46] demonstrated that WalkSAT easily outperforms RLSAT on hard instances. In the context of the Traveling Salesman problem (TSP), Joshi et al. [29] noted that GNNs can achieve promising results for relatively small instances, typically up to a few hundred cities. However, for instances involving millions of cities, the classical Lin-Kernighan-Helsgaun algorithm [27, 43] consistently finds solutions close to optimality. More recently, Liu et al. [35] demonstrated that learned heuristics still lag behind traditional solvers in effectively solving TSP. Regarding the MaxCut problem, Yao et al. [52] showed that a straightforward local search algorithm, Extremal Optimization [9], can outperform a specific GNN [13] across various configurations of dense and sparse random regular graphs. In contrast to our work, their study focused solely on random regular graphs and did not include comparisons with existing SOTA learned heuristics from the literature.

3 The MaxCut-Bench Benchmark

In this section, we introduce the datasets, distributions, and algorithms included in **MaxCut-Bench**.

3.1 Benchmark Datasets

We have curated a diverse collection of instances from both real-world datasets and random graph distributions to ensure a comprehensive and rigorous evaluation. To ensure a thorough comparison, we use commonly employed random graph models for instance generation, including Erdős et al. [18] (ER), Albert and Barabási [1] (BA), Holme and Kim [28] (HK), and Watts and Strogatz [49] (WS). For harder distributions, we use the following: Sherrington-Kirkpatrick (SK) spin glass [41], dense unweighted instances at their phase transitions [15], Physics [19], and the Stanford GSet dataset [53]. These harder instances have been employed for evaluating the performance of several SOTA traditional heuristics [7, 33, 32, 25]. Additional details regarding all mentioned datasets and the hyperparameters used for graph generation can be found in Appendix A.1. These datasets consist of graphs ranging in size from 70 to 2000 vertices.

3.2 Benchmark Algorithms

In this section, we give an overview of the different algorithms available in the benchmark. For more discussion of these algorithms, please refer to Appendix A.2. For our study, we consider both traditional and learning-based models. They can be organized into four categories.

Traditional Heuristics. These algorithms start with a candidate solution and then iteratively move to a neighboring solution by adding or removing a vertex. We provide implementations of the following algorithms: **Forward Greedy (FG)**, the traditional simple greedy heuristic that starts with an empty solution adds the largest gain to the candidate solution; **Reversible Greedy (RG)**, a variant of forward greedy that starts with a random solution and is also allowed to remove elements from the solution if gain in objective value can be obtained from such removal; **Tabu Search (TS)** [21], a modification of RG that avoids solutions previously seen to promote a more diverse search; and **Extremal optimization (EO)**[9], a stochastic local search algorithm.

Quantum Annealing (QA) Heuristics. These algorithms are designed to find the global minimum of an objective function within a set of potential solutions and are used mainly for problems where the search space is discrete (CO problems) with many local minima, such as finding the ground state of a spin glass or solving the traveling salesman problem. Since the MaxCut problem is equivalent to minimizing the Hamiltonian of a spin glass model [3], our benchmark supports two annealing algorithms, **Amplitude Heterogeneity Correction (AHA)** [33], and **Chaotic Amplitude Control (CAC)** [32]. We remark that none of the heuristics evaluated in this work exceed these QA heuristics in objective value; therefore, in the following we normalize by the best solution value found by one of these algorithms.

GNN-based heuristics. Khalil et al. [31] introduced **S2V-DQN**, which has become a highly influential work with thousands of citations. It may be thought as the forward greedy algorithm, except a GNN is used to select the next element to include. We reimplement this algorithm along with reversible extensions of S2V-DQN: **ECO-DQN** [4] and **LS-DQN** [51].

We include **Gflow-CombOpt** [55], a recently published spotlight work at NeurIPS 2023. This algorithm formulates CO problems as sequential decision-making sampling problems and designs efficient conditional Generative Flow Networks [6] to sample from the solution space and generate diverse solution candidates.

Finally, as MaxCut can easily be reduced to a constraint satisfaction problem, we include **RUN-CSP** [45] and **ANYCSP** [46]. These algorithms allows transitions between any two solutions in a single step.

4 Evaluation

In this section, we use the benchmark to investigate the **objective value**, **scalability** and **generalization** of algorithms by answering the following specific questions:

- For **objective value**, does combining deep learning with simple heuristics improve performance, or can the simple heuristics, with a much simpler model, do the heavy lifting (Section 4.1)? Secondly, can the learned heuristics outperform simple, general heuristics like Reversible Greedy and Tabu Search (Section 4.2)?
- For **generalization**, how well do these learning-based algorithms generalize beyond their training data on out-of-distribution instances (Section 4.3)?
- For **scalability**, how efficient are these algorithms in terms of time and space on large hard instances? Is the trade-off between complexity and performance reasonable (Section 4.4)?

All learned algorithms in our benchmark are implemented using PyTorch [37]. All experiments were conducted on a Linux server with a GPU (NVIDIA RTX A6000) and CPU (AMD EPYC 7713), using PyTorch 2.3.0, CIM [12], DGL 2.2.1 [48], and Python 3.11.9. We clearly state the changes necessary to update previous implementations and ensure that our reimplementations align with the results published in the literature. We provide all the details of these changes in Appendix A.4.

Evaluation settings. All training is performed on randomly 4000 generated graphs and the validation is performed on a fixed set of 50 held-out graphs from the same distribution. For synthetic datasets, testing is performed on 100 instances drawn from the same distribution; or upon the test instances provided in the original resource (see details in Appendix A.1). We evaluate the algorithms using the average approximation ratio as a performance metric. Given an instance, the approximation ratio for an algorithm is computed by normalizing the objective value of the best-known solution for the instance. As S2V-DQN and Forward Greedy are deterministic at test time, we use a single optimization episode for each graph. For all other algorithms, we run each algorithm for 50 randomly initialized episodes with $2|V|$ number of search steps per episode and select the best outcome from these runs following the experimental setup of Barrett et al. [4] and Yao et al. [51]. Experimentally, we have found that the performance of all algorithms saturates within this number of search steps (we refer the reader to the Appendix A.7 for more details).

4.1 Does deep learning really improve the performance of a traditional heuristic?

In this subsection, we address the question of whether the deep learning heuristics that combine a deep neural network with a traditional heuristic actually improve over the original heuristic.

S2V and LS-DQN. Specifically, the concept of S2V-DQN is exactly the Forward Greedy algorithm guided by a GNN. Similar to Forward Greedy, S2V-DQN begins with an empty solution and incrementally add a vertex to the solution until no greedy actions remain. The key distinction lies in how they select vertices: while Forward Greedy opts for the vertex that maximizes objective value increase, S2V-DQN delegates this decision to its GNN. Following in the footsteps of S2V-DQN, LS-DQN seeks to enhance vanilla Reversible Greedy. However, unlike vanilla RG, which halts when no greedy actions are left, LS-DQN incorporates the GNN to determine its termination criteria. Therefore, we seek to reproduce the results of Khalil et al. [31], Yao et al. [51], which show improvement over the respective traditional heuristic on a more limited selection of instances.

ECO-DQN. While S2V-DQN and LS-DQN use the current solution as the state-space representation for the reinforcement learning (RL) agent, ECO-DQN employs seven handcrafted features per vertex for its state space. Upon closer examination, we find that two of these features are closely related to the traditional heuristic, Tabu Search: **1) Marginal Gain:** the change in the objective value when a vertex is added to or removed from the solution set (we refer this action as a flip) **2) Time Since Flip:** steps since the vertex has been flipped to prevent short looping trajectories. To understand the connection between TS and ECO-DQN, we delve into how TS functions. Similar to ECO-DQN, TS starts with a random solution and iteratively explores the best neighboring solutions. To prevent revisiting local minima and explore the search space more effectively, TS employs a parameter known as tabu tenure, which acts as a short-term memory. This parameter restricts the repetition of the same actions for tabu tenure steps, preventing the algorithm from revisiting recent actions. Therefore, ECO-DQN uses a superset of the Tabu Search features to learn its agent.

To better understand the performance of ECO-DQN, we compare with an ablated version, which we call SoftTabu, which replaces the GNN with linear regression and omitting the features not related to TS, that is, all but the two features described above.

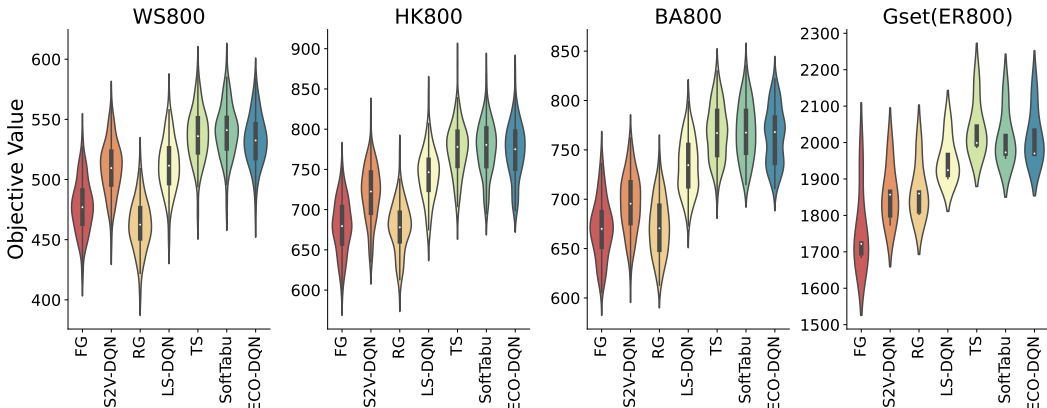


Figure 1: Violin plots of objective values of the learned and their classical counterparts on a selection of weighted instances.

Impact of the Findings. We evaluate these learned heuristics in various configurations on a wide range of graph distributions, with results shown in Table 1 and Figure 1. In summary, the GNN is shown to offer improvement when combined with the simpler classical heuristics Forward and Reversible Greedy; however, ECO-DQN fails to consistently improve on TS. In fact, the very simple heuristic TS outperforms all of the algorithms evaluated in this subsection. Next, we delve deeper to investigate the causes of some of the unexpected outcomes.

- **S2V-DQN.** From Table 1, it is evident that S2V-DQN (FG+GNN) significantly improves upon the Forward Greedy approach for the MaxCut problem, corroborating the empirical evaluation presented in the original work. This improvement is impressive, showing the promise of using GNNs to improve classical heuristics. However, we observe that TS, a simple and general heuristic with a single parameter, consistently outperforms S2V-DQN. In fact, even RG outperforms S2V-DQN on some distributions, such as ER (weighted and unweighted), BA (unweighted), Phase Transition networks among others, as shown in Table 1. This demonstrates how stochasticity is

Table 1: Performance comparison of learned heuristics with their simple counterparts (best in **bold**): The first and second halves of the table show results for unweighted and weighted instances, respectively.

Graph	Nodes	S2V-DQN		LS-DQN		ECO-DQN		
		FG	FG+GNN	RG	RG+GNN	TS	SoftTabu	ECO+GNN
GSet (ER)	800	0.970 \pm 0.003	0.970 \pm 0.001	0.985 \pm 0.001	0.992 \pm 0.001	0.999\pm0.001	0.996 \pm 0.001	0.997 \pm 0.001
GSet (Skew)	800	0.960 \pm 0.002	0.980 \pm 0.001	0.963 \pm 0.002	0.984 \pm 0.002	0.992\pm0.001	0.991 \pm 0.001	0.990 \pm 0.001
BA	800	0.938 \pm 0.007	0.951 \pm 0.006	0.952 \pm 0.003	0.983 \pm 0.003	0.992 \pm 0.002	0.993\pm0.002	0.991 \pm 0.002
WS	800	0.944 \pm 0.006	0.973 \pm 0.005	0.927 \pm 0.003	0.971 \pm 0.003	0.990 \pm 0.002	0.988 \pm 0.002	0.992\pm0.002
HK	800	0.939 \pm 0.007	0.966 \pm 0.005	0.951 \pm 0.003	0.984 \pm 0.003	0.992\pm0.002	0.992\pm0.002	0.992\pm0.002
Phase Transition	100-200	0.982 \pm 0.005	0.985 \pm 0.006	0.996 \pm 0.002	0.998 \pm 0.002	1.000\pm0.000	1.000\pm0.000	1.000\pm0.000
GSet (ER)	800	0.856 \pm 0.026	0.906 \pm 0.017	0.911 \pm 0.012	0.953 \pm 0.007	0.995\pm0.003	0.981 \pm 0.002	0.984 \pm 0.003
GSet (Skew)	800	0.863 \pm 0.030	0.890 \pm 0.027	0.871 \pm 0.013	0.942 \pm 0.007	0.980\pm0.005	0.975 \pm 0.005	0.966 \pm 0.009
GSet (Toroidal)	800	0.838 \pm 0.003	0.960 \pm 0.010	0.793 \pm 0.010	0.965 \pm 0.007	0.989 \pm 0.003	0.993 \pm 0.004	0.994\pm0.002
BA	800	0.853 \pm 0.018	0.886 \pm 0.019	0.855 \pm 0.012	0.934 \pm 0.011	0.978 \pm 0.007	0.979\pm0.008	0.972 \pm 0.009
WS	800	0.861 \pm 0.014	0.919 \pm 0.012	0.833 \pm 0.010	0.923 \pm 0.007	0.967 \pm 0.006	0.973\pm0.006	0.961 \pm 0.008
HK	800	0.857 \pm 0.019	0.908 \pm 0.017	0.855 \pm 0.012	0.937 \pm 0.009	0.977 \pm 0.007	0.978\pm0.008	0.974 \pm 0.009
Barrett et al. (ER)	200	0.866 \pm 0.038	0.951 \pm 0.024	0.954 \pm 0.014	0.987 \pm 0.010	1.000\pm0.001	1.000\pm0.001	1.000\pm0.001
Barrett et al. (BA)	200	0.849 \pm 0.054	0.937 \pm 0.043	0.903 \pm 0.039	0.977 \pm 0.032	0.984\pm0.032	0.984\pm0.032	0.983 \pm 0.033
SK spin-glass	70-100	0.865 \pm 0.057	0.939 \pm 0.049	0.994 \pm 0.010	0.999 \pm 0.003	1.000\pm0.000	1.000\pm0.000	1.000\pm0.000
Physics (Regular)	125	0.779 \pm 0.049	0.962 \pm 0.023	0.872 \pm 0.022	0.991 \pm 0.010	1.000\pm0.000	1.000\pm0.000	1.000\pm0.000

a powerful attribute when combined with local search. Khalil et al. [31] showed that the simple greedy approach, which starts with an empty solution and greedily moves the node that results in the largest improvement in cut weight, was the second-best competitor to S2V-DQN but did not compare it with RG.

- **ECO-DQN.** From Table 1, we observe that TS and SoftTabu often match or outperform ECO-DQN (ECO+GNN) in terms of performance. Similar to ECO-DQN, SoftTabu learns to strike a balance between exploration and exploitation. To ensure a fair comparison, we also used the publicly available datasets used to evaluate ECO-DQN in the original paper of Barrett et al. [4], which consists of ER and BA graphs.

In addition, we conducted all empirical experiments presented in ECO-DQN and compared them with TS and SoftTabu (additional results can be found in Appendix A.5). We found no significant difference in performance between ECO-DQN and its simpler counterparts. We conclude that the major contributing factors to solution quality can be achieved by the features related to TS with a simple model, and ECO-DQN does not gain any significant performance boost from being guided by a deep learning model. This underscores the importance of comparing an algorithm on a range of instances, as very small, synthetic generated datasets may lack the capability to effectively differentiate algorithm performance. In fact, adding the GNN adversely affects the generalization performance of ECO-DQN (as discussed in Section 4.3, Figure 3).

- **LS-DQN.** Our results support that LS-DQN enhances the performance of RG, as reported in Yao et al. [51]. However, our analysis contradicts the claim of Yao et al. [51] that LS-DQN matches the performance of ECO-DQN. This may be explained by observing that Yao et al. [51] compared the performance of ECO-DQN and LS-DQN only on complete graphs, which underscores the importance of comparing algorithms across a range of instances.

Final Considerations. In summary, adding a GNN to a traditional heuristic showed an improvement in the cases of Forward Greedy and Reversible Greedy. However, the authors of ECO-DQN added enough features to the algorithm to enable learning something similar to TS, and the GNN does not add any additional improvement over TS and may in fact hurt the performance.

4.2 Have deep learning heuristics obtained any absolute improvement over the best traditional heuristic?

In this section, we evaluate the algorithms to assess whether any of the deep learning heuristics can achieve the SOTA objective value on the instances in the MaxCut benchmark. While it may be too early to expect learned heuristics to beat SOTA heuristics tailored for specific problems, the question of how learned heuristics fare against general heuristics remains unanswered. One of the main reasons for this is the variety of baselines and instances used in existing work (more details can be found in Appendix A.3).

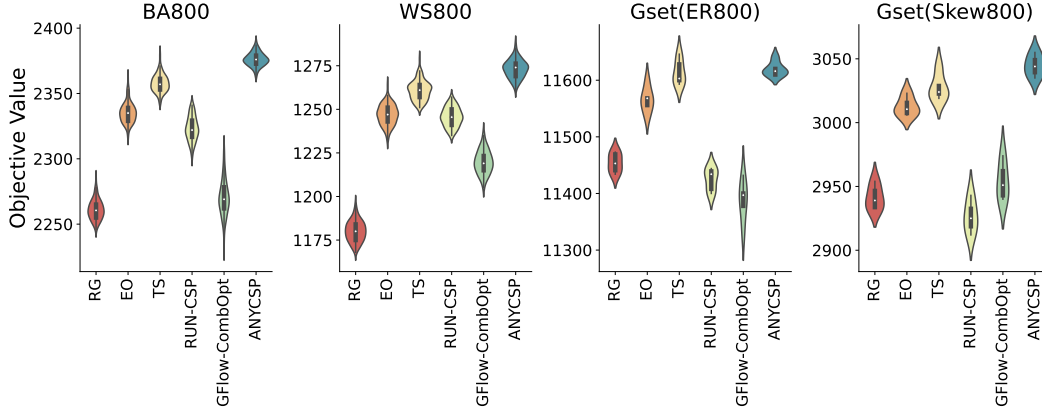


Figure 2: Violin plots of objective values of the learned and classical heuristics on a selection of unweighted instances.

Table 2: Average Approximation ratios of classical and learned heuristics (best in **bold**); “—” denotes no reasonable result is achieved by the corresponding algorithm and the first and second halves of the table show results for unweighted and weighted instances, respectively.

Graph	Nodes	Classical Heuristics			Learned Heuristics		
		RG	EO	TS	RUN-CSP	GFlow-CombOpt	ANYCSP
GSet (ER)	800	0.985±0.001	0.995±0.001	0.999±0.001	0.982±0.001	0.979±0.003	0.999±0.000
GSet (Skew)	800	0.963±0.002	0.987±0.000	0.992±0.001	0.958±0.003	0.967±0.003	0.997±0.001
BA	800	0.952±0.003	0.983±0.003	0.992±0.002	0.978±0.003	0.955±0.006	1.000±0.000
WS	800	0.927±0.003	0.979±0.003	0.990±0.002	0.978±0.003	0.958±0.004	0.999±0.000
HK	800	0.951±0.003	0.983±0.003	0.992±0.002	0.977±0.003	0.930±0.015	1.000±0.000
Phase Transition	100-200	0.996±0.002	0.999±0.001	1.000±0.000	0.994±0.002	0.993±0.004	1.000±0.000
<hr/>							
GSet (ER)	800	0.911±0.012	0.973±0.005	0.995±0.003	0.909±0.007	—	0.998±0.002
GSet (Skew)	800	0.871±0.013	0.954±0.007	0.980±0.005	0.925±0.013	—	0.995±0.005
GSet (Torodial)	800	0.793±0.010	0.948±0.010	0.989±0.003	0.976±0.002	—	0.999±0.002
BA	800	0.855±0.012	0.949±0.008	0.978±0.007	0.931±0.009	—	1.000±0.000
WS	800	0.833±0.010	0.943±0.007	0.967±0.006	0.950±0.007	—	0.999±0.000
HK	800	0.855±0.012	0.949±0.009	0.977±0.007	0.937±0.009	—	1.000±0.000
Barrett et al. (ER)	200	0.954±0.014	0.989±0.008	1.000±0.001	0.940±0.015	—	1.000±0.000
Barrett et al. (BA)	200	0.903±0.039	0.969±0.035	0.984±0.032	0.958±0.035	—	0.986±0.032
SK spin-glass	70-100	0.994±0.010	0.995±0.006	1.000±0.000	0.962±0.019	—	1.000±0.001
Physics (Regular)	125	0.872±0.022	0.986±0.011	1.000±0.000	0.989±0.009	—	1.000±0.000

Impact of findings. We compare GFlow-CombOpt, RUN-CSP, and ANYCSP with the traditional heuristics RG, EO, and TS. We observe that deep learning-based solutions can often be outperformed, especially on larger instances. Next, we discuss the insights that our empirical observations can provide for each algorithm.

- **GFlow-CombOpt.** We restrict our empirical evaluation of GFlow-CombOpt to unweighted instances because Zhang et al. [55] only evaluated GFlow-CombOpt for MaxCut on unweighted BA graphs, following Sun et al. [42], and our attempt to adapt GFlow-CombOpt to handle weighted graphs (details in Appendix A.4) performed poorly and did not surpass the Forward Greedy baseline. From Table 2 and Figure 2, TS and EO consistently outperform GFlow-CombOpt. Moreover, surprisingly, RG exceeds the performance of GFlow-CombOpt on four of the six distributions tested, including unweighted BA graphs. In our opinion, this example showcases the need for more standardization of evaluation, as GFlow-CombOpt is outperformed more often than not by a naive greedy heuristic.
- **RUN-CSP.** From Table 2, we observe that TS outperforms RUN-CSP on all distributions, EO outperforms RUN-CSP on most distributions, while RUN-CSP outperforms RG in most, but not all, distributions. Although Toenshoff et al. [45] included hard unweighted instances from the Gset dataset, they showed RUN-CSP obtains superior performance to a Semidefinite Programming (SDP) solver based on dual scaling [14]. SDP-based approaches typically underperform in practice

for MaxCut [31, 51], even with extended computation times. Although these approaches have the highest theoretical approximation ratio, they are easy to beat in practice. Again, this underscores the need for carefully chosen baselines to demonstrate improvement.

- **ANYCSP.** We analyze ANYCSP in its default configuration and observe that it consistently finds near-optimal solutions (that is, solutions near the value found by the Quantum Annealing algorithms), and superior in value to TS and the other traditional local search algorithms. These promising results demonstrate that ANYCSP can effectively learn the solution structure across diverse graph distributions and remains robust across multiple distributions .

Final considerations. The empirical findings suggest that benchmarking against weak heuristics on a very particular set of instances may establish a low standard, potentially leading to a misleading sense of achievement. Hence, selecting appropriate baselines is crucial to accurately assess the effectiveness of learned heuristics. At a minimum, we recommend that any work should at least include RG, and ideally TS, as a baseline – failure to consistently beat the naive RG baseline suggests that the algorithm may need further development.

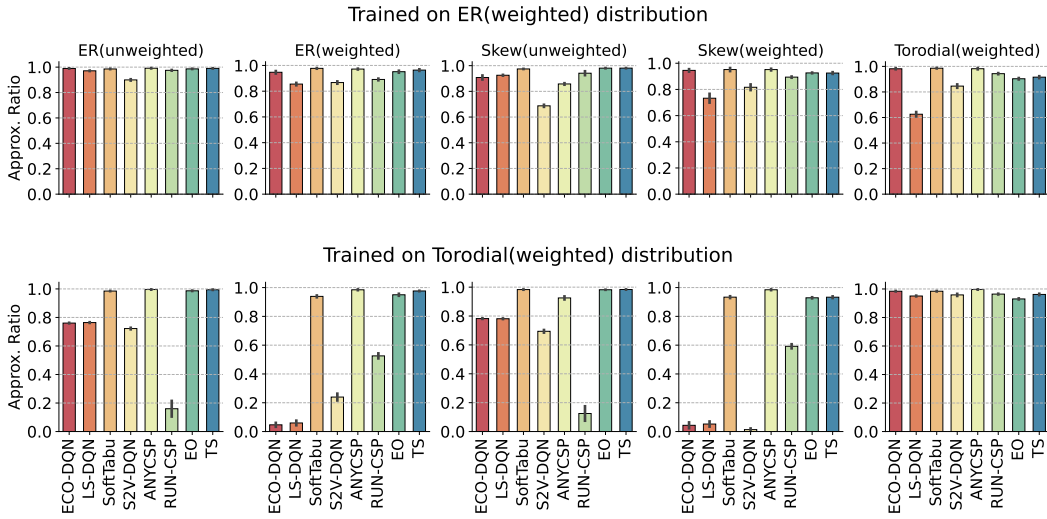


Figure 3: Generalisation of agents to unseen graph sizes and structures.

4.3 Generalization: Do learned heuristics generalizes well on unseen distributions?

The ability of learned heuristics to perform well on a wide range of distributions, even if these distributions are not represented during training, is a highly desirable characteristic for practical CO problems [11]. Many works include experiments to assess how well an the heuristic generalizes. Often, this is in the form of training on smaller instances and generalizing to test on larger ones, although cross-distribution performance is also frequently assessed.

Several learned heuristics such as ECO-DQN, LS-DQN, and S2V-DQN are claimed to exhibited promising performance across a diverse range of graph structures, including those not present in their training data. In this section, we evaluate the generalization performance using **MaxCut-Bench**.

Impact of Findings. From Figure 3, we notice that there can be a substantial decline in performance when the learned heuristics are tested on graph distributions other than train distributions, with the notable exception of ANYCSP. In particular, observe that when trained on the torodial distribution (second row), the test performance of ECO-DQN, LS-DQN, S2V-DQN, and RUN-CSP may fall below 25% on several distributions. This outcome may be anticipated. Intuitively, we would expect a network trained on instances of a particular structure to adapt toward this class of instances and perform poorer for different structures. We observe that TS, SoftTabu and EO seem to be generalize well across wider distributions. Both TS and EO has a single parameter, which we optimized for the training distribution to assess its generalization performance.

These results raise the possibility that the generalization of learned heuristics from learning over small and easy instances to testing on larger and more complicated ones may not be as robust as the literature

[31, 4, 5, 51] suggests. This feature is often touted as an amelioration of the expensive training process required for the learned heuristics. We provide additional results on our generalization experiments in A.6.

4.4 Efficiency and scalability analysis

In this section, we analyze the efficiency and scalability of learned heuristics over ER graphs of size $|V| = 800$ from Gset dataset. For time efficiency, we evaluate the efficiency of the algorithms by measuring the wall-clock time. For scalability, we evaluate average GPU and CPU usage per second of these learned algorithms.

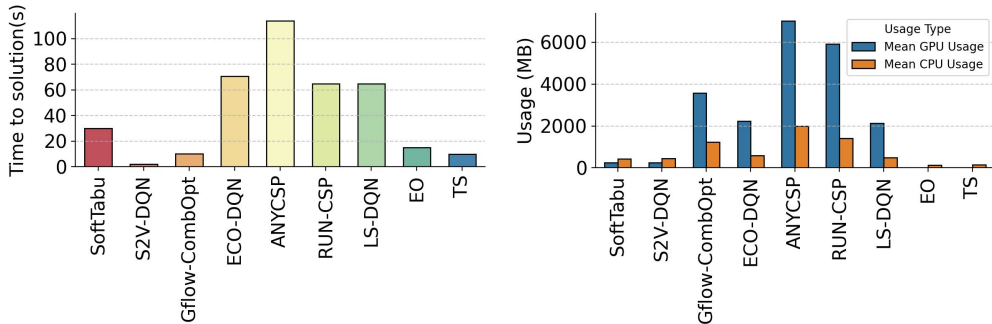


Figure 4: Comparison of the wall-clock time and average GPU and CPU memory utilization among heuristics.

Impact of Findings. From Figure 4, we observe that algorithms that use multiple randomly initialized episodes require significantly more time and memory. We observe that ANYCSP takes the longest time to complete and consumes the most memory, whereas classical heuristics are faster by an order of magnitude.

5 Conclusion and Future Directions

In this paper, we introduce **MaxCut-Bench**, a comprehensive benchmark for evaluating deep learning-based algorithms for the Maximum Cut problem, consisting of carefully selected instance distributions and implemented algorithms. It is our intent that **MaxCut-Bench** will foster further research and refinement of learning-based algorithms, enabling more informed evaluations and comparisons. We regard our work as a long-term evolving project and are dedicated to its continuous development. Our roadmap for the future includes expanding its scope to cover a broader spectrum of CO problems, incorporating more cutting-edge models, and integrating newer and more challenging distributions of instances.

While one might expect that extensively tailored heuristics can outperform learned approaches, our empirical findings suggest that simple local search heuristics frequently outperform complicated GNN-based heuristics. Specifically, Tabu Search, a local search heuristic that tries to avoid solutions previously encountered, outperforms all but one of the evaluated learned heuristics across a broad range of instance distributions. Even more surprising, we found that a naive reversible greedy algorithm RG is not consistently outperformed by several learned heuristics, including highly cited ones such as S2V-DQN. In addition, we showed that ablating the GNN from ECO-DQN did not hurt its performance, and showed evidence that ECO-DQN may simply be learning a heuristic similar to Tabu Search. On the positive side, ANYCSP did show a modest improvement over Tabu Search, although it uses many times the computational resources. Further, we observed that in some cases using a GNN to guide a traditional heuristic can improve the performance of the original heuristic.

References

- [1] Albert, R. and Barabási, A.-L. (2002). Statistical mechanics of complex networks. *Reviews of modern physics*, 74(1):47.
- [2] Angelini, M. C. and Ricci-Tersenghi, F. (2023). Modern graph neural networks do worse than classical greedy algorithms in solving combinatorial optimization problems like maximum independent set. *Nature Machine Intelligence*, 5(1):29–31.
- [3] Barahona, F., Grötschel, M., Jünger, M., and Reinelt, G. (1988). An application of combinatorial optimization to statistical physics and circuit layout design. *Operations Research*, 36(3):493–513.
- [4] Barrett, T., Clements, W., Foerster, J., and Lvovsky, A. (2020). Exploratory combinatorial optimization with reinforcement learning. In *Proceedings of the AAAI conference on artificial intelligence*, volume 34, pages 3243–3250.
- [5] Barrett, T. D., Parsonson, C. W., and Laterre, A. (2022). Learning to solve combinatorial graph partitioning problems via efficient exploration. *arXiv preprint arXiv:2205.14105*.
- [6] Bengio, E., Jain, M., Korablyov, M., Precup, D., and Bengio, Y. (2021). Flow network based generative models for non-iterative diverse candidate generation. *Advances in Neural Information Processing Systems*, 34:27381–27394.
- [7] Benlic, U. and Hao, J.-K. (2013). Breakout local search for the max-cut problem. *Engineering Applications of Artificial Intelligence*, 26(3):1162–1173.
- [8] Bilbro, G., Mann, R., Miller, T., Snyder, W., van den Bout, D., and White, M. (1988). Optimization by mean field annealing. *Advances in neural information processing systems*, 1.
- [9] Boettcher, S. and Percus, A. G. (2001). Extremal optimization for graph partitioning. *Physical Review E*, 64(2):026114.
- [10] Böther, M., Kißig, O., Taraz, M., Cohen, S., Seidel, K., and Friedrich, T. (2022). What’s wrong with deep learning in tree search for combinatorial optimization. *arXiv preprint arXiv:2201.10494*.
- [11] Cappart, Q., Chételat, D., Khalil, E. B., Lodi, A., Morris, C., and Veličković, P. (2023). Combinatorial optimization and reasoning with graph neural networks. *Journal of Machine Learning Research*, 24(130):1–61.
- [12] Chen, F., Isakov, B., King, T., Leleu, T., McMahon, P., and Onodera, T. (2022). cim-optimizer: a simulator of the Coherent Ising Machine.
- [13] Chen, Z., Li, X., and Bruna, J. (2017). Supervised community detection with line graph neural networks. *arXiv preprint arXiv:1705.08415*.
- [14] Choi, C. and Ye, Y. (2000). Solving sparse semidefinite programs using the dual scaling algorithm with an iterative solver. *Manuscript, Department of Management Sciences, University of Iowa, Iowa City, IA*, 52242.
- [15] Coppersmith, D., Gamarnik, D., Hajiaghayi, M., and Sorkin, G. B. (2004). Random max sat, random max cut, and their phase transitions. *Random Structures & Algorithms*, 24(4):502–545.
- [16] Cplex, I. I. (2009). V12. 1: User’s manual for cplex. *International Business Machines Corporation*, 46(53):157.
- [17] Elsokkary, N., Khan, F. S., La Torre, D., Humble, T. S., and Gottlieb, J. (2017). Financial portfolio management using d-wave quantum optimizer: The case of abu dhabi securities exchange. Technical report, Oak Ridge National Lab.(ORNL), Oak Ridge, TN (United States).
- [18] Erdős, P., Rényi, A., et al. (1960). On the evolution of random graphs. *Publ. math. inst. hung. acad. sci.*, 5(1):17–60.
- [19] Festa, P., Pardalos, P. M., Resende, M. G., and Ribeiro, C. C. (2002). Randomized heuristics for the max-cut problem. *Optimization methods and software*, 17(6):1033–1058.

- [20] Fujishige, S. (2005). *Submodular functions and optimization*. Elsevier.
- [21] Glover, F. (1990). Tabu search: A tutorial. *Interfaces*, 20(4):74–94.
- [22] Goemans, M. X. and Williamson, D. P. (1995). Improved approximation algorithms for maximum cut and satisfiability problems using semidefinite programming. *Journal of the ACM (JACM)*, 42(6):1115–1145.
- [23] Goto, H., Tatsumura, K., and Dixon, A. R. (2019). Combinatorial optimization by simulating adiabatic bifurcations in nonlinear hamiltonian systems. *Science advances*, 5(4):eaav2372.
- [24] Gurobi Optimization, LLC (2023). Gurobi Optimizer Reference Manual.
- [25] Hamerly, R., Inagaki, T., McMahon, P. L., Venturelli, D., Marandi, A., Onodera, T., Ng, E., Langrock, C., Inaba, K., Honjo, T., et al. (2019). Experimental investigation of performance differences between coherent ising machines and a quantum annealer. *Science advances*, 5(5):eaau0823.
- [26] Helmberg, C. and Rendl, F. (2000). A spectral bundle method for semidefinite programming. *SIAM Journal on Optimization*, 10(3):673–696.
- [27] Helsgaun, K. (2000). An effective implementation of the lin–kernighan traveling salesman heuristic. *European journal of operational research*, 126(1):106–130.
- [28] Holme, P. and Kim, B. J. (2002). Growing scale-free networks with tunable clustering. *Physical review E*, 65(2):026107.
- [29] Joshi, C. K., Cappart, Q., Rousseau, L.-M., and Laurent, T. (2020). Learning the travelling salesperson problem requires rethinking generalization. *arXiv preprint arXiv:2006.07054*.
- [30] Karalias, N. and Loukas, A. (2020). Erdos goes neural: an unsupervised learning framework for combinatorial optimization on graphs. *Advances in Neural Information Processing Systems*, 33:6659–6672.
- [31] Khalil, E., Dai, H., Zhang, Y., Dilkina, B., and Song, L. (2017). Learning combinatorial optimization algorithms over graphs. *Advances in neural information processing systems*, 30.
- [32] Leleu, T., Khoystatee, F., Levi, T., Hamerly, R., Kohno, T., and Aihara, K. (2021). Scaling advantage of chaotic amplitude control for high-performance combinatorial optimization. *Communications Physics*, 4(1):266.
- [33] Leleu, T., Yamamoto, Y., McMahon, P. L., and Aihara, K. (2019). Destabilization of local minima in analog spin systems by correction of amplitude heterogeneity. *Physical review letters*, 122(4):040607.
- [34] Li, Z., Chen, Q., and Koltun, V. (2018). Combinatorial optimization with graph convolutional networks and guided tree search. *Advances in neural information processing systems*, 31.
- [35] Liu, S., Zhang, Y., Tang, K., and Yao, X. (2023). How good is neural combinatorial optimization? a systematic evaluation on the traveling salesman problem. *IEEE Computational Intelligence Magazine*, 18(3):14–28.
- [36] Lourenço, H. R., Martin, O. C., and Stützle, T. (2003). Iterated local search. In *Handbook of metaheuristics*, pages 320–353. Springer.
- [37] Paszke, A., Gross, S., Massa, F., Lerer, A., Bradbury, J., Chanan, G., Killeen, T., Lin, Z., Gimelshein, N., Antiga, L., et al. (2019). Pytorch: An imperative style, high-performance deep learning library. *Advances in neural information processing systems*, 32.
- [38] Perdomo-Ortiz, A., Dickson, N., Drew-Brook, M., Rose, G., and Aspuru-Guzik, A. (2012). Finding low-energy conformations of lattice protein models by quantum annealing. *Scientific reports*, 2(1):1–7.
- [39] Schuetz, M. J., Brubaker, J. K., and Katzgraber, H. G. (2022). Combinatorial optimization with physics-inspired graph neural networks. *Nature Machine Intelligence*, 4(4):367–377.

- [40] Selman, B., Kautz, H. A., Cohen, B., et al. (1993). Local search strategies for satisfiability testing. *Cliques, coloring, and satisfiability*, 26:521–532.
- [41] Sherrington, D. and Kirkpatrick, S. (1975). Solvable model of a spin-glass. *Physical review letters*, 35(26):1792.
- [42] Sun, H., Guha, E. K., and Dai, H. (2022). Annealed training for combinatorial optimization on graphs. *arXiv preprint arXiv:2207.11542*.
- [43] Taillard, É. D. and Helsgaun, K. (2019). Popmusic for the travelling salesman problem. *European Journal of Operational Research*, 272(2):420–429.
- [44] Tiunov, E. S., Ulanov, A. E., and Lvovsky, A. (2019). Annealing by simulating the coherent ising machine. *Optics express*, 27(7):10288–10295.
- [45] Toenshoff, J., Ritzert, M., Wolf, H., and Grohe, M. (2021). Graph neural networks for maximum constraint satisfaction. *Frontiers in artificial intelligence*, 3:580607.
- [46] Tönshoff, J., Kisin, B., Lindner, J., and Grohe, M. (2022). One model, any csp: Graph neural networks as fast global search heuristics for constraint satisfaction. *arXiv preprint arXiv:2208.10227*.
- [47] Venturelli, D. and Kondratyev, A. (2019). Reverse quantum annealing approach to portfolio optimization problems. *Quantum Machine Intelligence*, 1(1-2):17–30.
- [48] Wang, M. Y. (2019). Deep graph library: Towards efficient and scalable deep learning on graphs. In *ICLR workshop on representation learning on graphs and manifolds*.
- [49] Watts, D. J. and Strogatz, S. H. (1998). Collective dynamics of ‘small-world’ networks. *nature*, 393(6684):440–442.
- [50] Yamamoto, Y., Aihara, K., Leleu, T., Kawarabayashi, K.-i., Kako, S., Fejer, M., Inoue, K., and Takesue, H. (2017). Coherent ising machines—optical neural networks operating at the quantum limit. *npj Quantum Information*, 3(1):49.
- [51] Yao, F., Cai, R., and Wang, H. (2021). Reversible action design for combinatorial optimization with reinforcement learning. *arXiv preprint arXiv:2102.07210*.
- [52] Yao, W., Bandeira, A. S., and Villar, S. (2019). Experimental performance of graph neural networks on random instances of max-cut. In *Wavelets and Sparsity XVIII*, volume 11138, pages 242–251. SPIE.
- [53] Ye, Y. (2003). The gset dataset. <https://web.stanford.edu/yye/yye/Gset/>.
- [54] Yolcu, E. and Póczos, B. (2019). Learning local search heuristics for boolean satisfiability. *Advances in Neural Information Processing Systems*, 32.
- [55] Zhang, D., Dai, H., Malkin, N., Courville, A., Bengio, Y., and Pan, L. (2023). Let the flows tell: Solving graph combinatorial optimization problems with gflownets. *arXiv preprint arXiv:2305.17010*.

A Appendix

A.1 Detailed Description of Datasets

In this section, we provide details on the datasets, groups of datasets, and random graphs models used in this paper.

- **Erdős-Rényi (ER).** This well-known random graph model by Erdős et al. [18] connects each pair of vertices with a probability p . For ease of comparison with the experiments in ECO-DQN paper, we set the same parameters from the paper and generate graphs of size $|V| = 200$ using $p = 0.15$ with edge weights $w \in \{0, \pm 1\}$ for training and validation. For testing, we use 100 test graphs from this distribution that were used for evaluating ECO-DQN.
- **Barabási-Albert (BA).** The random graph model by Albert and Barabási [1] iteratively adds nodes, connecting them to m already existing nodes. For our experiments, we generate graphs of size $|V| = 800$ using $m = 4$, with edge weights $w \in \{0, \pm 1\}$ and $w \in \{0, 1\}$. For ease of comparison with the experiments in ECO-DQN paper, we also generate graphs of size $|V| = 200$ using $m = 4$ with edge weights $w \in \{0, \pm 1\}$ for training and validation, following Barrett et al. [4]. For testing, we use 100 test graphs with 200 vertices, which were used for evaluating ECO-DQN.
- **Holme-Kim (HK).** The random graph model by Holme and Kim [28], similar to the BA model, includes an extra step for each randomly created edge that forms a triangle with probability p . We generate graphs of size $|V| = 800$ using $m = 4$ and $p = 0.10$, with edge weights $w \in \{0, \pm 1\}$ and $w \in \{0, 1\}$.
- **Watts-Strogatz (WS).** The random graph model by Watts and Strogatz [49] starts with a well-structured ring lattice with a mean degree of k . In the next step, each edge is replaced with probability p by another edge sampled uniformly at random. This approach aims to preserve "small-world properties" while maintaining a random structure similar to ER graphs. We generate graphs of size $|V| = 800$ using $k = 4$ and $p = 0.15$, with edge weights $w \in \{0, \pm 1\}$ and $w \in \{0, 1\}$.
- **GSet.** This dataset [53] is extensively used to benchmark classical heuristics [7, 33, 32] for MaxCut. The dataset comprises three types of weighted and unweighted random graphs: ER graphs with uniform edge probabilities, skew graphs with decaying connectivity, and regular toroidal graphs. For generating training and validation distributions, we use the independent graph generator Rudy by Giovanni Rinaldi, which is used for generating GSet graphs as sourced from Ye [53]. For training and validation, we generate ER graphs of size $|V| = 800$ with $p = 0.06$, union of planar graphs (skew graphs) of size $|V| = 800$ with density $d = 0.99$ and regular toroidal graphs of size $|V| = 800$ for training and validation. The arguments for generating the graphs with Rudy are collected from Helmberg and Rendl [26].
- **Physics.** This distribution comes from a publicly available library of MaxCut instances¹ and includes synthetic and realistic instances that are widely used in the optimization community (see references at the library website). For training and validation, we generate a similar distribution, and for testing, we make use of a subset of the instances available, namely ten problems from Ising Spin. glass models in physics (the first 10 instances in Set2 of the library) following Khalil et al. [31]. All ten instances have 125 nodes and 375 edges, with edge weights $w \in \{0, \pm 1\}$.
- **Sherrington-Kirkpatrick spin glass.** This distribution contains dense Sherrington-Kirkpatrick instances with elements $J_{ij} \in \{-1, 1\}$ generated from ER graphs based on examples from Hamerly et al. [25]. We generate graphs of size 70 to 100 vertices for training and validation. For testing, we use instances with the best known value provided in CIM-Optimizer [12].
- **Phase transition.** This distribution contains dense unweighted instances from ER graphs at the phase transition ($p = 0.5$) [15], based on examples from Hamerly et al. [25]. We generate graphs with 100 to 200 vertices for training and validation and make use of test instances provided in CIM-Optimizer [12].

A.2 Detailed Description of Benchmark Algorithms

All algorithms make use of 50 attempts, and the best solution found is reported. The exceptions are FG and S2V-DQN, which both are deterministic and start from the empty set. Next, we provide details about each algorithm discussed in our paper.

Traditional Heuristics.

¹<https://grafo.etsii.urjc.es/opticom/index.php.html>

- **Forward Greedy (FG)**. The algorithm starts with an empty solution and greedily adds vertices to the solution that result in the greatest immediate increase in the objective value until no further improvements can be made. It does not allow reversible actions, meaning it does not remove any vertex from the solution once added.
- **Reversible Greedy (RG)**. The algorithm starts with an arbitrary solution and either adds or removes a vertex, taking the action with the largest possible non-negative gain to the objective value. If all gains are negative, the algorithm terminates.
- **Tabu Search (TS)**. The algorithm starts with an arbitrary solution and strategically flips the membership of vertices (include/exclude from the solution set) at each step to improve the objective value. It incorporates a mechanism called tabu tenure, where, after flipping the membership of a vertex, the vertex will be marked as tabu (forbidden) for a certain period of steps to prevent the immediate reversal of the flip and encourage exploration of new areas. At each step, it flips a vertex that is not marked as tabu and results in the greatest increase in objective value. Despite being marked as tabu, a vertex can still be flipped if it leads to the best objective value discovered so far. Unlike forward and reversible greedy algorithms, this algorithm continues searching for a fixed number of iterations even when no further immediate improvements can be made, thus enhancing the search process by exploring a broader solution space and potentially finding better solutions over time. Various improved versions of this algorithm have been proposed [21]; we consider the vanilla version of the algorithm (see Algorithm 1). Further details can be found in Glover [21].

Algorithm 1 Tabu Search

Require: oracle f , graph $G(V, E)$, initial solution S_0 , tabu tenure γ , maximum iterations $maxiter$

```

1: Initialize current solution  $S \leftarrow S_0$ 
2: Initialize tabu list  $T$  as an empty dictionary
3: Initialize best objective value  $bestobj \leftarrow f(S)$ 
4: Initialize iteration counter  $iter \leftarrow 0$ 
5: while  $iter < maxiter$  do
6:    $bestmove \leftarrow \text{None}$ 
7:    $bestvalue \leftarrow -\infty$ 
8:   for each vertex  $v \in V$  do
9:     Flip the membership of  $v$  in  $S$  to obtain  $S'$ 
10:    Calculate objective value  $f(S')$ 
11:    if  $f(S') > bestobj$  or ( $v \notin T$  and  $f(S') > bestvalue$ ) then
12:       $bestmove \leftarrow v$ 
13:       $bestvalue \leftarrow f(S')$ 
14:    end if
15:  end for
16:  Flip the membership of  $bestmove$  in  $S$ 
17:  Add/update  $bestmove$  in tabu list  $T$  with tabu tenure  $\gamma$ 
18:  if  $f(S) > bestobj$  then
19:     $bestobj \leftarrow f(S)$ 
20:  end if
21:  for each vertex  $v$  in tabu list  $T$  do
22:    Decrease tabu tenure of  $v$  by 1
23:    if tabu tenure of  $v$  is 0 then
24:      Remove  $v$  from  $T$ 
25:    end if
26:  end for
27:  Increment iteration counter  $iter \leftarrow iter + 1$ 
28: end while
29: return  $bestobj$ 

```

- **Extremal optimization (EO)**. The algorithm begins with an initial arbitrary solution and sorts the vertices by their descending marginal gain. It then defines a probability distribution $P_k \propto k^{-\tau}$ where $1 \leq k \leq |V|$ for a given value of the parameter τ to determine the likelihood of selecting each vertex based on its rank in the sorted list. At each step, an index k is selected according to this probability distribution, and the membership of the selected vertex is flipped. This method allows the algorithm to escape local optima and explore the search space more effectively, thereby

increasing the chances of finding better solutions. Similar to TS, it stops after a fixed number of iterations (see Algorithm 2). Further details can be found in Boettcher and Percus [9].

Algorithm 2 Extremal Optimization Algorithm

Require: oracle f , graph $G(V, E)$, initial solution S_0 , tau τ , maximum iterations $maxiter$

```

1: Initialize current solution  $S \leftarrow S_0$ 
2: Initialize a probability distribution  $P_k \propto k^{-\tau}$  where  $1 \leq k \leq |V|$ 
3: Initialize best objective value  $bestobj \leftarrow f(S)$ 
4: Initialize iteration counter  $iter \leftarrow 0$ 
5: while  $iter < maxiter$  do
6:   Initialize a list  $marginal\_gains \leftarrow []$ 
7:   for each vertex  $v \in V$  do
8:     Flip the membership of  $v$  in  $S$  to obtain  $S'$ 
9:     Calculate objective value  $f(S')$ 
10:    Calculate  $gain \leftarrow f(S') - f(S)$ 
11:    Append  $gain$  to  $marginal\_gains$ 
12:   end for
13:   Sort vertices in descending order of marginal gains
14:   Select an index  $k$  according to the probability distribution  $P_k$ 
15:   Select the vertex  $v_k$  that is in the  $k$ -th position in the sorted list
16:   Flip the membership of  $v_k$  in  $S$  to obtain new solution  $S$ 
17:   if  $f(S) > bestobj$  then
18:      $bestobj \leftarrow f(S)$ 
19:   end if
20:   Increment iteration counter  $iter \leftarrow iter + 1$ 
21: end while
22: return  $bestobj$ 

```

GNN-based heuristics

- **S2V-DQN.** Similar to FG, the algorithm starts from an empty solution and incrementally constructs solutions by adding one vertex at each step to the current solution, guided by a GNN. Once a vertex is added to the solution, it cannot be removed; in other words, the algorithm does not reverse its earlier decisions. The state space of its RL agent is represented by the current solution. The algorithm stops when no action can improve the objective value. The reward function of the algorithm is simply the change in the objective value. Further details can be found in Khalil et al. [31].
- **ECO-DQN.** Unlike S2V-DQN, this algorithm starts with an arbitrary partition of vertices and allows reversible actions. Barrett et al. [4] provides seven handcrafted features per node to represent the state space of its RL agent. At each step, it selects a vertex and flips its membership. The RL agent often chooses vertices that do not correspond to the greatest immediate increase in the objective value (non-greedy). Thus, it aims to strike a balance between exploitation and exploration of the search space. The algorithm stops after a fixed number of iterations. It provides a reward to the RL agent only when a new solution has been found, which equals the difference between the new best solution and the previous best solution. Since the reward can be very sparse, the algorithm also provides a small intermediate reward to the agent when the agent reaches a new locally minimal solution. Further details can be found in Barrett et al. [4].
- **LS-DQN.** Similar to RG, LS-DQN allows reversible actions and starts with an arbitrary solution instead of an empty one. The state space of its RL agent is represented by the current solution. At each step, it selects a vertex and flips the membership of the selected vertex. It stops after a fixed number of iterations or can terminate on its own. The reward function of this algorithm is defined as the negative value change of the objective function at each step. It generalizes to a variety of CO problems, like MaxCut and TSP. Further details can be found in Yao et al. [51].
- **Gflow-CombOpt.** The algorithm begins with an empty solution. The formulation of the Markov decision process (MDP) for the generative flow network proceeds as follows: at each step, it adds one vertex to the solution. After each action, it checks if adding the vertex would decrease the cut value. If so, it excludes the vertex, ensuring it is never added back to the solution. Despite starting with an empty solution, the algorithm generates diverse solution candidates by sampling from a

probability distribution in a sequential decision-making process. Further details can be found in Zhang et al. [55].

- **RUN-CSP.** The algorithm solves CO problems that can be mapped to binary constraint satisfaction problems (CSP). It employs a graph neural network as a message-passing protocol, with the CSP instances modeled as a graph where nodes correspond to variables and edges represent constraints. Like other GNN-based heuristics, it is not a reinforcement learning approach; rather, the loss function to optimize this algorithm is designed to satisfy as many constraints as possible. The results show that it performs effectively on significantly larger instances, even when trained on relatively small ones. Further details can be found in Toenshoff et al. [45].
- **ANYCSP.** The algorithm is an end-to-end search heuristic for any constraint satisfaction problem. Tönshoff et al. [46] introduced a novel representation of CSP instances, called the constraint value graph, which allows for direct processing of any CSP instance. The state space of RL agent is represented by both the current solution and the best solution found so far. At each step, the algorithm generates a soft assignment of variables within the CSP instance, enabling transitions between any two solutions in a single step. To encourage exploration and prevent the search from getting stuck in local maxima, a reward scheme similar to ECO-DQN is employed. Notably, the RL agent does not receive a reward upon reaching an unseen local minimum. Empirical evidence has shown that this approach can compete with or even surpass classical SOTA problem-specific heuristics. Further details can be found in Tönshoff et al. [46].

Quantum Annealing

Quantum annealing algorithms start by framing the optimization problem as an energy landscape of a quantum system, with the solution being the state of the lowest energy. Initially, the quantum system is set in a superposition of all possible solutions, which represents a high-energy state. The objective is to steer the system towards the lowest energy state, which corresponds to the optimal or near-optimal solution for the problem. Next, we describe two SOTA quantum annealing algorithms used in our benchmark

- **Amplitude Heterogeneity Correction (AHC).** The algorithm maps the objective function of CO problems to the energy landscape of a physical system called Coherent Ising Machine [50]. It relaxes the binary vertex states of MaxCut problem to continuous values and find low energy states efficiently. It finds solutions of better or equal quality for GSet instances compared to those previously known from the classical SOTA heuristic Breakout Local Search [7].
- **Chaotic Amplitude Control (CAC).** To improve the scalability, this algorithm make use of nonrelaxational dynamics that can accelerate the sampling of low energy states to reduce the time to find optimal solutions . Futher details can be found in Leleu et al. [32].

A.3 Baseline and Instance Bias

In this section, we continue our discussion on the lack of consensus regarding instances and baselines. This inconsistency leads to a situation where empirical results in different research papers are often not comparable. From Figure 5, we observe that only a handful of learned local heuristics, such as ECO-DQN and RUN-CSP, compare with SOTA classical heuristics. This highlights potential baseline biases in the current research landscape. Similarly, in Figure 6, few heuristics actually evaluate their performance on hard instances that are used to benchmark SOTA heuristics. Next, we discuss the evaluation specifics for each of the learning-based algorithms.

- **S2V-DQN.** As previously noted, Khalil et al. [31] demonstrated that a simple greedy approach, which moves a vertex from one side of the cut to the other if that action results in the greatest improvement in cut weight, is the second-best performer after S2V-DQN. Despite the well-known poor performance of this approach [20] for MaxCut, we observe a lack of comparisons with simple enhancements to the greedy approach, such as iterated local search [36], TS and EO. Furthermore, other baselines like CPLEX and SDP approaches perform poorly, especially on large instances in practice, even with a longer cut-off time [31, 4].
- **ECO-DQN.** Although ECO-DQN included several SOTA simulated annealing heuristics in their evaluation, they did not compare ECO-DQN with TS, the closest classical algorithm ECO-DQN resembles. Moreover, in terms of generalization, they only considered the ER distribution of the GSet. We find that the generalization performance of ECO-DQN can significantly degrade when tested on other distributions of the GSet (more details in Table 7).

- **LS-DQN.** The performance of LS-DQN was evaluated on weighted complete graphs of various sizes, excluding standard hard instances typically used for benchmarking SOTA heuristics. This raises the possibility that on an arbitrary distribution, LS-DQN can achieve comparable performance to SOTA heuristics, while weaker baselines may struggle. Classical baselines, such as SDP and genetic algorithms, exhibited poorer performance compared to RG in the empirical evaluation of LS-DQN. However, there is a noticeable absence of comparisons with straightforward enhancements over RG. Given that LS-DQN aims to improve upon RG, it is crucial to include simple baselines that enhance the performance of RG.
- **RUN-CSP.** While Toenshoff et al. [45] included unweighted instances from the GSet distribution to evaluate GSet, our empirical evaluation indicates that both classical and learned heuristics struggle more with optimizing weighted instances compared to unweighted ones. This suggests that weighted instances pose greater optimization challenges. Evaluating the algorithm in these instances would provide a clearer understanding of its performance.
- **Gflow-CombOpt.** As mentioned earlier, Zhang et al. [55] evaluated GFlow-CombOpt for MaxCut exclusively on unweighted BA graphs, following the Sun et al. [42]. These instances are neither theoretically known to be hard nor commonly used to assess the empirical performance of SOTA classical heuristics. Additionally, baselines such as Mean Field Annealing (MFA) [8], Erdos Goes Neural [30] and Sun et al. [42], lack empirical evidence supporting their effectiveness as heuristics for MaxCut. While Gurobi is a leading heuristic for integer programming, it often requires significant time to find an optimal solution [55]. Consequently, depending on the cutoff time applied, the best-known solution for each instance can vary considerably.
- **ANYCSP.** Similar to RUN-CSP, the performance of this algorithm was evaluated on unweighted instances from the GSet distribution and compared with SOTA learned heuristics. However, classical simple heuristics were not included in the comparison, leaving it unclear whether ANYCSP can demonstrate superior performance over the simpler algorithms.

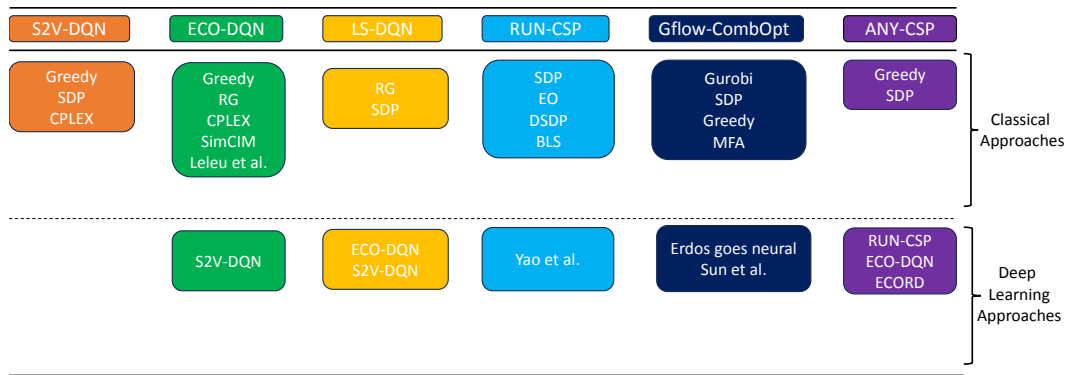


Figure 5: Researchers often select arbitrary baselines, which, when combined with instance bias, can lead to confusion in empirical evaluations.

A.4 Reproducibility

In this section, we list all the changes we made to the previous implementations of algorithms and provide implementation details of the algorithms.

A.4.1 S2V-DQN

We use the publicly available implementation of S2V-DQN by Barrett et al. [4] as our initial code-base² for implementing S2V-DQN. This implementation had poor scalability because it used dense representations of graphs. It also could not handle distributions containing graphs of different sizes because dense representations of graphs of different sizes cannot be batched together. Therefore, we reimplement it to ensure it can scale up easily to larger instances. To ensure a fair comparison, we evaluate the performance of our implementation against pretrained models provided by Barrett et al. [5] and provide the results in Table 4.

²Code available at: <https://github.com/tomdbar/eco-dqn>

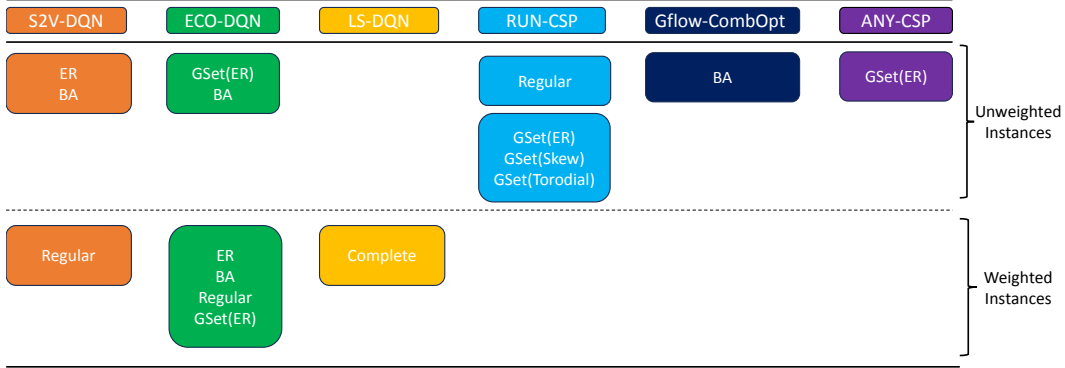


Figure 6: Researchers evaluate their proposed learned heuristics on a diverse range of weighted and unweighted distributions for MaxCut. These instances may pose a challenge for weak baselines while potentially being relatively manageable for learned heuristics.

A.4.2 ECO-DQN

Similar to S2V-DQN, we use the publicly available implementation of ECO-DQN and make similar improvements as we did for S2V-DQN. To ensure reproducibility, we compare our implementation with the pretrained networks provided by Barrett et al. [4] and report the results in Table 4.

A.4.3 LS-DQN

Since the LS-DQN codebase was not publicly available initially, we contacted the authors. Unfortunately, their codebase³ is designed specifically for clustered graphs and is not suitable for training on arbitrary graph distributions. The authors did not provide details about their configuration and hyper-parameter settings in the paper. However, we were able to replicate similar improvements over RG using the GNN, as reported in the paper (see Table 1).

A.4.4 GFlow-CombOpt

For unweighted instances, we utilize the original implementation⁴ of GFlow-CombOPT with the default configuration. For weighted instances, we incorporate weighted graph convolution to utilize edge weights and make necessary adjustments to ensure that a vertex is added to the solution set only if it improves the cut value compared to not including it. However, we observe poor empirical performance of the algorithm for weighted instances. Therefore, we restrict our empirical evaluation of GFlow-CombOPT to unweighted instances.

A.4.5 RUN-CSP and ANYCSP

We use the PyTorch implementation of RUN-CSP⁵ and ANYCSP⁶ with the default configuration.

A.4.6 CAC and AHC

We use the implementations of these two algorithms provided by Chen et al. [12] and tune their hyperparameters using Bayesian Optimization Hyperband.

A.4.7 TS

To tune the value of tabu tenure, we run a grid search with a step size of 10, starting from 20 to 150, over the validation dataset and use the tuned tabu tenure for testing. We report the parameters used for our experiments in Table 3.

³Code available at: <https://github.com/MingzheWu418/LocalSearch-DQN>

⁴Code available at: <https://github.com/zdhNarsil/GFlowNet-CombOpt>

⁵Code available at: <https://github.com/toenshoff/RUNCSP-PyTorch>

⁶Code available at: <https://github.com/toenshoff/ANYCSP>

Table 3: Parameters used for Tabu Search (TS) and Extremal Optimization (EO).

Graph	Nodes	Tabu Tenure (TS)	Tau (EO)
Gset (ER)	800	80	1.4
GSet (Skew)	800	90	1.4
BA	800	110	1.3
WS	800	140	1.4
HK	800	100	1.4
Phase Transition	100-200	20	1.8
GSet (ER)	800	30	1.7
GSet (Skew)	800	90	1.4
GSet (Torodial)	800	100	1.4
BA	800	120	1.2
WS	800	110	1.3
HK	800	110	1.2
Barrett et al. (ER)	200	10	1.9
Barrett et al. (BA)	200	20	1.6
SK spin-glass	70-100	20	1.8
Physics (Regular)	125	20	1.4

A.4.8 EO

To tune the value of tau, we run a grid search with a step size of 0.1, starting from 1.1 to 1.9, over the validation dataset and use the tuned tau for testing. We report the parameters used for our experiments in Table 3.

A.5 Additional results on ECO-DQN

The best-known solutions for the datasets used to evaluate ECO-DQN, along with the pretrained models with weights, are publicly available. We use this data to compare our results with the pretrained models and those presented in the original paper. However, for BA60, we were unable to load the pre-trained model for S2V-DQN. From Table 4, we observe that our implementation has achieved similar empirical performance. It is worth noting that for some experiments (e.g., BA200, ER100), we were unable to reproduce the results of S2V-DQN and ECO-DQN from the paper (see Table 4 in the original paper) using our implementation and pretrained models.

Table 4: The approximation ratios, averaged across 100 graphs for each graph structure and size.

Graph	Our Implementation				Literature		Pretrained	
	ECO-DQN	S2V-DQN	SoftTabu	TS	ECO-DQN	S2V-DQN	ECO-DQN	S2V-DQN
ER20	0.99	0.97	0.99	1.00	0.99	0.97	0.99	0.97
ER40	1.00	0.97	1.00	1.00	1.00	0.99	1.00	0.98
ER60	1.00	0.97	1.00	1.00	1.00	0.99	1.00	0.97
ER100	1.00	0.93	1.00	1.00	1.00	0.98	1.00	0.92
ER200	1.00	0.95	1.00	1.00	1.00	0.96	1.00	0.95
BA20	1.00	0.98	1.00	1.00	1.00	0.97	1.00	0.97
BA40	1.00	0.97	1.00	1.00	1.00	0.98	1.00	0.96
BA60	1.00	0.97	1.00	1.00	1.00	0.98	1.00	-
BA100	1.00	0.96	1.00	1.00	1.00	0.97	1.00	0.95
BA200	0.98	0.94	0.98	0.98	1.00	0.96	0.98	0.93

Next, we revisit the generalization experiments in the original paper and report the results in Tables 5 and 6. We observe that there is no significant performance difference between TS, SoftTabu, and ECO-DQN; they all perform reasonably well. We would also like to highlight that the generalization performance of ECO-DQN presented in the paper is somewhat inconclusive due to the lack of harder instances. Specifically, these instances may be too simple compared to the GSet instances we use for our generalization experiments, making it possible for ECO-DQN to solve them without requiring

any special efforts. However, the performance of S2V-DQN significantly drops as the size of the graphs increases. Similar results have been reported in Barrett et al. [4].

Table 5: Generalization of agents trained on ER graphs of size $|V| = 40$ to unseen graph sizes and structures.

Graph	TS	SoftTabu	S2V-DQN	ECO-DQN
ER60	1.00	1.00	0.97	1.00
ER100	1.00	1.00	0.96	1.00
ER200	1.00	1.00	0.95	1.00
ER500	0.99	0.99	0.92	0.99
BA40	1.00	1.00	0.97	1.00
BA60	1.00	1.00	0.97	1.00
BA100	1.00	1.00	0.94	1.00
BA200	0.98	0.98	0.86	0.98
BA500	0.96	0.98	0.74	0.97

Finally, we tested agents trained on weighted ER graphs with $|V| = 200$ on real-world datasets and hard instances, following the experimental setup of Barrett et al. [4]. We extended the empirical experiments of ECO-DQN by including distributions other than the ER distribution. From Table 7, we observe that SoftTabu outperforms ECO-DQN, except for ER graphs where ECO-DQN performs slightly better than SoftTabu.

A.6 Additional results on generalization

Due to space constraints, we present the results of the generalization of learned and classical heuristics that are trained on a skewed graph distribution of size $|V| = 800$ from GSet and tested on various distributions of size $|V| = 2000$ from GSet. From Figure 7, we observe that simple heuristics match or outperform the performance of learned heuristics.

Final Considerations. We conclude that our implementation complies with the original implementation of ECO-DQN and conclude that ECO-DQN does not provide any significant performance boost when guided by a GNN rather than a simple linear regression.

A.7 Additional details on Evaluation settings

Since we are using the previous codebase from several works, and they are not equally optimized, we use the number of search steps instead of a timeout. As both S2V-DQN and Gflow-CombOpt are irreversible (only add to the solution set), these algorithms can run for a maximum of $|V|$ steps. For other learned algorithms, we run the experiments for $4|V|$ steps and find no significant improvement in the objective value. We present the results of the learned heuristics in Table 8.

Table 6: Generalization of agents trained on BA graphs of size $|V| = 40$ to unseen graph sizes and structures.

Graph	Tabu	SoftTabu	S2V-DQN	ECO-DQN
ER40	1.00	1.00	0.97	1.00
ER60	1.00	1.00	0.95	1.00
ER100	1.00	1.00	0.94	1.00
ER200	1.00	1.00	0.93	0.99
ER500	1.00	0.99	0.90	0.98
BA60	1.00	1.00	0.96	1.00
BA100	1.00	1.00	0.94	1.00
BA200	0.98	0.98	0.81	0.98
BA500	0.97	0.99	0.50	0.99

Table 7: Average approximation ratios on known benchmarks: The second half of the table shows results for extended experiments.

Dataset	Type	Nodes	Tabu	SoftTabu	S2V-DQN	ECO-DQN
Physics	Regular	125	1.000	1.000	0.928	1.000
G1-10	ER	800	0.989	0.984	0.950	0.990
G22-31	ER	2000	0.953	0.977	0.919	0.981
G11-G13	Torodial	800	0.951	0.988	0.919	0.984
G14-G21	Skew	800	0.960	0.973	0.752	0.940
G32-34	Torodial	2000	0.915	0.983	0.923	0.969
G35-42	Skew	2000	0.949	0.965	0.694	0.864

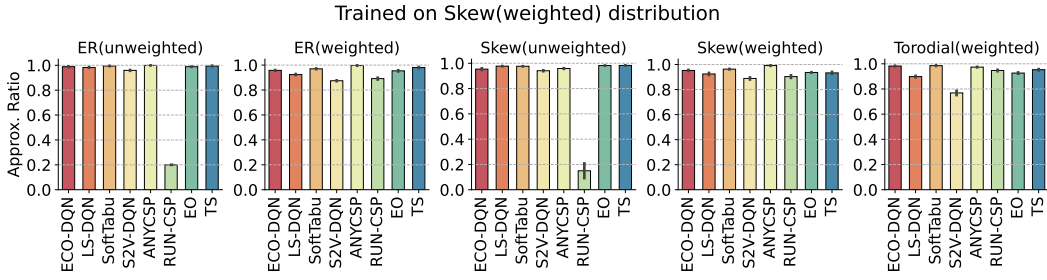


Figure 7: Generalization of agents to unseen graph sizes and structures.

Table 8: Average approximation ratios of learned heuristics optimized for $4|V|$ steps: The first and second halves of the table show results for unweighted and weighted instances, respectively.

Graph	Nodes	ECO-DQN	LS-DQN	RUN-CSP	ANYCSP
Gset (ER)	800	0.997 ± 0.001	0.993 ± 0.001	0.979 ± 0.002	0.999 ± 0.000
GSet (Skew)	800	0.989 ± 0.001	0.983 ± 0.002	0.954 ± 0.001	0.997 ± 0.001
BA	800	0.992 ± 0.002	0.983 ± 0.003	0.980 ± 0.002	1.000 ± 0.000
WS	800	0.992 ± 0.002	0.972 ± 0.003	0.979 ± 0.003	1.000 ± 0.000
HK	800	0.991 ± 0.002	0.983 ± 0.003	0.979 ± 0.003	1.000 ± 0.000
Phase Transition	100-200	1.000 ± 0.000	0.998 ± 0.001	0.984 ± 0.005	1.000 ± 0.000
GSet (ER)	800	0.981 ± 0.006	0.950 ± 0.008	0.912 ± 0.009	0.998 ± 0.002
GSet (Skew)	800	0.967 ± 0.008	0.946 ± 0.018	0.914 ± 0.018	0.995 ± 0.005
GSet (Torodial)	800	0.992 ± 0.004	0.964 ± 0.003	0.974 ± 0.002	0.999 ± 0.002
BA	800	0.973 ± 0.008	0.933 ± 0.010	0.937 ± 0.009	1.000 ± 0.000
WS	800	0.961 ± 0.007	0.922 ± 0.008	0.954 ± 0.007	1.000 ± 0.000
HK	800	0.975 ± 0.009	0.937 ± 0.009	0.944 ± 0.007	1.000 ± 0.000
Barrett et al. (ER)	200	1.000 ± 0.001	0.988 ± 0.008	0.945 ± 0.012	1.000 ± 0.000
Barrett et al. (BA)	200	0.983 ± 0.031	0.977 ± 0.032	0.960 ± 0.016	0.989 ± 0.037
SK spin-glass	70-100	1.000 ± 0.000	0.999 ± 0.002	0.962 ± 0.019	1.000 ± 0.001
Physics (Regular)	125	1.000 ± 0.000	0.995 ± 0.009	0.982 ± 0.008	1.000 ± 0.000